JOURNAL OF VIROLOGY, Aug. 2000, p. 7238–7249 Vol. 74, No. 16
0022-538X/00/$04.00+0

Mapping and Characterization of the N-Terminal I Domain of Human Immunodeficiency Virus Type 1 $Pr55^{Gag}$

STEPHANIE SANDEFUR, RITA M. SMITH, VASUNDHARA VARTHAKAVI, AND PAUL SPEARMAN*

Departments of Pediatrics and Microbiology and Immunology, Vanderbilt University School of Medicine, Nashville, Tennessee

Received 18 January 2000/Accepted 22 May 2000

Human immunodeficiency virus (HIV) type 1 particles assemble at the plasma membrane of cells in a manner similar to that of the type C oncoretroviruses. The $Pr55^{Gag}$ molecule directs the assembly process and is sufficient for particle assembly in the absence of all other viral gene products. The I domain is an assembly domain that has been previously localized to the nucleocapsid (NC) region of Gag. In this study we utilized a series of Gag-green fluorescent protein (GFP) fusion proteins to precisely identify sequences that constitute the N-terminal I domain of $Pr55^{Gag}$. The minimal sequence required for the I domain was localized to the extreme N terminus of NC. Two basic residues (arginine 380 and arginine 384) within the initial seven residues of NC were found to be critical for the function of the N-terminal I domain. The presence of positive charge alone in these two positions, however, was not sufficient to mediate the formation of dense Gag particles. The I domain was required for the formation of detergent-resistant complexes of Gag protein, and confocal microscopy demonstrated that the I domain was also required for the formation of punctate foci of Gag proteins at the plasma membrane. Electron microscopic analysis of cells expressing Gag-GFP fusion constructs with an intact I domain revealed numerous retrovirus-like particles (RVLPs) budding from the plasma membrane, while I domain-deficient constructs failed to generate visible RVLPs. These results provide evidence that Gag-Gag interactions mediated by the I domain play a central role in the assembly of HIV particles.

Human immunodeficiency virus (HIV) particle assembly takes place at the plasma membrane of infected cells. $Pr55^{Gag}$ is a polyprotein precursor derived from the HIV *gag* gene that forms the major core components of the virus particle. $Pr55^{Gag}$, when expressed in the absence of all other viral components, is sufficient to generate retrovirus-like particles (RVLPs) which bud from the plasma membrane in a manner essentially identical to that of infectious virions. The Gag polyprotein thus contains sufficient intrinsic capacity to allow its transport from cytoplasmic sites of translation to the plasma membrane, where it engages additional Gag molecules, interacts with plasma membrane components, and directs the particle budding process (10, 19, 32, 37). The viral protease is activated during the budding process and subsequently cleaves $Pr55^{Gag}$ into the following components (listed in order of their occurrence from N to C terminus): matrix (MA), capsid (CA), spacer peptide 1 (SP1), nucleocapsid (NC), spacer peptide 2 (SP2), and p6. Three assembly domains which are common to the Gag polyproteins of lentiviruses, oncoretroviruses, and spumaviruses have been described. The membrane interaction (M) domain is required for transport to and interaction with the plasma membrane of cells. In the case of most retroviral Gag proteins, including HIV, the M domain requires a myristic acid modification of the N-terminal glycine residue of Gag acting in concert with a series of basic amino acids located within the MA region (17, 42). Some retroviruses, such as Rous sarcoma virus (RSV), lack the myristic acid modification of MA yet still have a functional M domain which is located within the N-terminal two-thirds of MA (8, 34, 38). The interaction (I) domain is a functional domain required for the assembly of particles of normal density (1.16 to 1.18 g/ml) (12, 27). This domain is located within NC and is present in at least two copies in the case of HIV and RSV (1). The late (L) domain is required for particle budding and is a determinant of retroviral particle size (13, 27). When L domain function is abrogated in the context of a full-length provirus, particles are generated normally at the plasma membrane of transfected cells but are inefficiently released (16).

While the M, I, and L domains represent distinct assembly domains within retroviral Gag polyproteins, additional assembly functions within HIV type 1 (HIV-1) Gag are located outside of these domains. The CA region contains a dimerization domain which has been shown to be essential for Gag-Gag interaction when in vitro assembly systems are employed (15, 36, 39). Some point mutations within the major homology region (MHR) of HIV-1 CA create severe defects in assembly (23), and numerous mutations within CA positioned C terminal to the MHR that result in elimination or severe reduction of particle assembly have been described previously (7, 20, 28, 35, 40). Thus, the domains designated M, I, and L are useful for conserved functional retroviral assembly domains but do not encompass all necessary assembly functions located within HIV-1 $Pr55^{Gag}$.

The I domain of HIV Gag was first localized to the NC region by Bennett and coworkers, who demonstrated that two distinct fragments of HIV-1 NC could restore dense particle formation to an RSV Gag molecule which by itself resulted in the formation of only light-density particles (1). Their work established that the I domain is conserved functionally among retroviral Gag proteins and that it is redundant within NC. I domains have more recently been described for murine leukemia virus and for human foamy virus (2). Although the HIV-1 NC fragments initially report to contain a functional I domain each contained a zinc finger motif, it is clear that a zinc finger is not required for I domain function. This is best exemplified by the demonstration that human foamy viruses, which contain no zinc finger motif, have at least two identifiable I domains (2). At the same time, it was demonstrated that the addition of a simple string of basic residues could reconstitute I domain

* Corresponding author. Mailing address: Pediatric Infectious Diseases, Vanderbilt University, D-7235 MCN, Nashville, TN 37232-2581. Phone: (615) 322-2250. Fax: (615) 343-9723. E-mail: paul.spearman@mcmail.vanderbilt.edu.

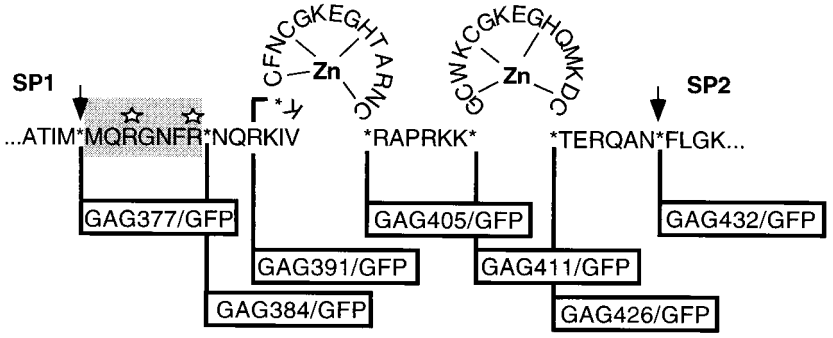

FIG. 1. Schematic representation of Gag-GFP constructs subdividing HIV-1 NC. Asterisks indicate the sites of Gag truncation and GFP fusion. The number represents the C-terminal amino acid residue expressed, with the Gag initiator methionine considered residue 1. The shaded box highlights the minimum sequence required for I domain function as discussed in the text. The stars indicate the two key arginine residues (R380 and R384) that were mutated to abrogate the function of the N-terminal I domain, creating the series of N-terminal I domain mutant constructs. Note that the constructs containing the double arginine-to-alanine mutation are designated by the number of the residue at the truncation site (GFP fusion site) followed by the designation R380/384A in parentheses. For example, GAG405/GFP containing the double arginine-to-alanine mutation is designated GAG405(R380/384A)/GFP. Arrows, HIV protease cleavage sites.

function in the context of an I domain-deficient RSV Gag molecule. Members of our group have demonstrated that the HIV-1 I domain does not require the presence of a zinc finger motif and that I domain function in the context of serially C-terminally truncated Gag proteins is localized to the N-terminal subdomain of NC (29). Two additional findings correlated closely with the mapping of the I domain by particle density determination: (i) the efficiency of Gag protein membrane binding and (ii) a peripheral, punctate localization of Gag within cells, as seen by confocal microscopy. These studies suggested to us that a further understanding of the I domain may provide important additional insights into the mechanisms of HIV particle assembly.

In this study, we sought to identify more precisely the residues within the N-terminal subdomain of NC which are required for I domain function, as well as to define the contribution of downstream sequences of NC in the context of N-terminal I domain mutations. The N-terminal I domain was mapped to the extreme N-terminal seven amino acids of NC, and two key arginine residues were identified. Although this small sequence is sufficient to reconstitute normal particle density, additional sequences within the N-terminal subdomain, first zinc finger, basic linker region, and second zinc finger enhance I domain function, as indicated by quantitative subcellular fractionation analysis and confocal microscopic analysis.

MATERIALS AND METHODS

Construction of plasmids expressing Gag-GFP fusion proteins. The Gag coding sequence for all constructs was derived from the HXB2gpt proviral clone. The construction of expression plasmids for the fusion proteins designated 55GAG/GFP, MACA/GFP, GAG377/GFP, GAG391/GFP, GAG405/GFP, GAG411/GFP, and MA/GFP has been previously described (29). Additional Gag-green fluorescent protein (GFP) constructs were constructed for the purposes of this study. The GFP sequence was taken from plasmid pEGFP-N1, pEGFP-N2, or pEGFP-N3 (Clontech, Palo Alto, Calif.). Plasmid pTM1 was used as the backbone expression plasmid for all constructs. All of the *gag* gene fragments, except 55GAG(R380,384A)/GFP, were generated via PCR using primers that introduced an *Nco*I site at the 5′ ATG site and a *Bam*HI site at the 3′ fusion site. The resulting PCR fragments were ligated into pTM1, using the *Nco*I and *Bam*HI sites found in the polylinker region. GFP cassettes were then digested with *Bam*HI-*Not*I and ligated into *Bam*HI-*Eag*I-digested intermediate Gag constructs to generate fusions in the appropriate reading frame. All PCR-generated *gag* gene fragments were verified to be correct by sequencing of the complete *gag* gene insert within the expression plasmid. The expression plasmid design allows for the expression of full-length MA fused to GFP (MA/GFP), full-length Gag fused to GFP (55GAG/GFP), a GFP fusion at the end of the SP1 region between CA and NC (GAG377/GFP), and a series of Gag-GFP fusions created at serial sites within the NC region (GAG384/GFP, GAG391/GFP, GAG405/GFP, GAG411/GFP, GAG426/GFP, and GAG432/GFP). The number in each construct designation represents the most C-terminal *gag* codon present, with the numbering beginning with the *gag* initiator ATG. Fusion breakpoints within NC are illustrated diagrammatically in Fig. 1.

Oligonucleotides used in the construction of the Gag expression plasmids described above were AGAGCCATGGGTGCGAGAGCGTCAGTA [forward primer for all Gag-GFP constructs except 55GAG(R380,384A)/GFP], CGCGG ATCCCGTAATTTTGGCTGACCTGATT (reverse primer for MA/GFP), CGGG ATCCATTATGGTAGCTGAATTTG (reverse primer for Gag377/GFP), CGG GATCCTAAAATTGCCTCTCTGCAT (reverse primer for Gag384/GFP), GGT GGATCCCTTAACAATCTTTCTTTG (reverse primer for Gag391/GFP), GGTG GATCCGCAATTTCTGGCTGTGTG (reverse primer for Gag405/GFP), GGTG GATCCCTTTTTCCTAGGGGCCCTG (reverse primer for Gag411/GFP), GGTGGATCCACAATCTTTCATTTGGTGTCC (reverse primer for Gag426/GFP), and GCGGATCCATTAGCCTGTCTCTCAGTACAATCTTTCATTTG GTG (reverse primer for Gag432/GFP).

Construction of plasmids expressing Gag-GFP fusion proteins containing amino acid mutations within the N-terminal I domain. Arginine 380 and arginine 384 were mutated to alanine in the context of 55GAG/GFP using overlap-extension PCR with the following primers: ATAATGATGCAGGCCGGCAAT TTTGCGAACCAAAGAAAG [inside forward primer for 55GAG(R380,384A)/GFP], TTTCTTTGGTTCGCAAAATTGCCGGCCTGCATCATTATG [inside reverse primer for 55GAG(R380,384A)/GFP], AAGCTGCAGAATGGGATAG [outside forward primer for 55GAG(R380,384A)/GFP], and CCAGATCTTCC CTAAAAAATTAGC [outside reverse primer for 55GAG(R380,384A)/GFP]. The final PCR product was digested with *Pst*I and *Bgl*II and ligated into 55GAG/GFP to create the 55GAG(R380,384A)/GFP plasmid. These same mutations were then generated in the context of the GAG384/GFP construct. In addition, the two arginine codons were individually mutated (R380A and R384A), and lysine was substituted for both residues (R380,384K). This was achieved using a PCR reaction with HXB2gpt as the template, the forward primer listed in the section above, and the following reverse primers: CGGGATCCGCAAAATTG CCGGCCTGCATCATTATGGTAGC [reverse primer for GAG384(R380,384A)/GFP], CGGGATCCTAAAATTGCCGGCCTGCATCATTATGGTAGC [reverse primer for GAG384(R380A)/GFP], CGGGATCCGCAAAATTGCCTCT CTGCATACATTATGGTAGC [reverse primer for GAG384(R384A)/GFP], and GCGGATCCCTTAAAATTGCCTTTCTGCATCATTATGGTAGC [reverse primer for GAG384(R380,384K)/GFP]. Generation of the NC constructs containing the double arginine-to-alanine mutations with sequential addition of NC subdomains was then accomplished via PCR using the 55GAG(R380,384A)/GFP plasmid as a template and the reverse primers listed above for construction of the sequential fusion sites within NC.

Expression of Gag-GFP fusion proteins. The vaccinia virus-T7 RNA polymerase system was used to express Gag-GFP fusion proteins in the African green monkey kidney cell line BSC-40 as previously described (29–31). T7 RNA polymerase was provided by infection of the cells with 10 PFU of the recombinant vaccinia virus VTF 7-3 per cell. Following infection, cells were transfected with the appropriate plasmid using a liposome-mediated transfection protocol.

Equilibrium density measurements of Gag-GFP pseudovirion particles. Gag-GFP fusion proteins were produced in BSC-40 cells as described above. Culture medium was removed 3 to 4 h posttransfection and replaced with Dulbecco's modified Eagle medium deficient in cysteine and methionine and supplemented with 75 μCi of [^{35}S]cysteine-methionine per ml. Following an overnight incubation, supernatants were collected, filtered through a 0.45-μm-pore-size syringe filter, layered on a 20% sucrose cushion in NTE (100 mM NaCl, 10 mM Tris-Cl [pH 8.0], 1 mM EDTA), and subjected to centrifugation at 100,000 × *g* for 3 h.

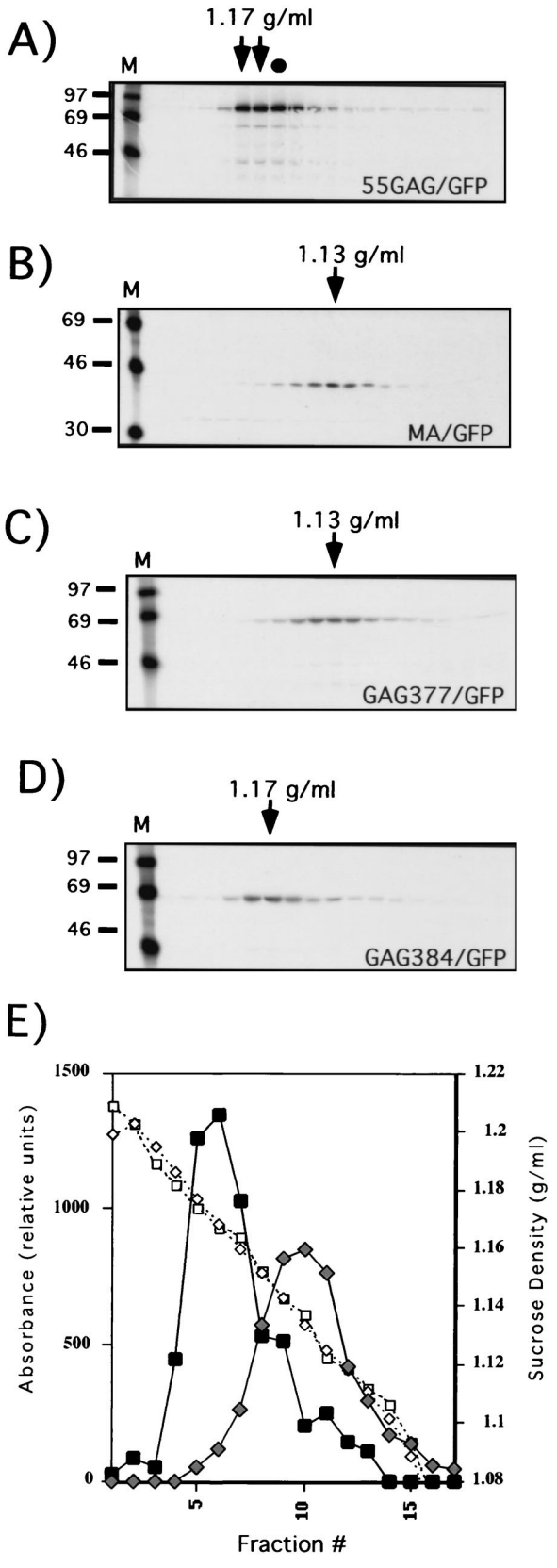

FIG. 2. Equilibrium density of Gag-GFP particles defining the N-terminal I domain. (A) 55GAG/GFP; (B) MA/GFP; (C) GAG377/GFP; (D) GAG384/GFP. Following overnight labeling with [^{35}S]cysteine-methionine, supernatants were collected, layered on a 20% sucrose cushion, and subjected to centrifugation. Pelleted material was layered on top of a linear 20 to 60% sucrose gradient and centrifuged to equilibrium. Twenty equal fractions were collected, immunoprecipitated using pooled HIV-positive patient sera, and analyzed by SDS-PAGE followed by autoradiography. The densities of the peak fractions are indicated above each autoradiogram by the arrow(s). Lanes M, molecular mass markers (molecular mass in kilodaltons is indicated at the left of each autoradiogram in panels A to D). The closed circle in panel A is above the lane containing a fraction with a density of 1.16 g/ml. (E) Plot of densitometry results and sucrose densities representing the autoradiograms of panels C and D. Black squares, relative absorbance of bands seen in the GAG384/GFP autoradiogram; grey diamonds, relative absorbance of bands seen in the Gag377/GFP autoradiogram; open squares, sucrose densities of the fractions in the GAG377/GFP experiment; open diamonds, sucrose densities of fractions from the GAG384/GFP experiment. Relative absorbance values were obtained by scanning the autoradiograms shown in panels B and C, followed by pixel quantitation with National Institutes of Health Image software (version 1.61).

The medium and cushion were removed; the pelleted material was resuspended in NTE and layered on the top of a linear 20 to 60% (wt/vol) sucrose gradient. The gradient was subjected to centrifugation at 100,000 × *g* for 16 to 20 h, after which 20 equal fractions were collected. The precise refractive index of each fraction was determined using a refractometer, which allowed calculation of the sucrose density of each fraction. The remainder of the fractions were immunoprecipitated using pooled HIV-positive patient sera and separated via sodium dodecyl sulfate-polyacrylamide gel electrophoresis (SDS-PAGE), followed by autoradiographic analysis. Each gradient presented is representative of a minimum of two gradient fractionations, in which the peak densities shown were identical.

Subcellular fractionation and quantitation of protein. BSC-40 cells grown in 100-mm^3 plates and expressing Gag-GFP fusion proteins were harvested 16 h posttransfection and processed for differential sedimentation centrifugation as previously described (29). Briefly, cells from one dish were subjected to Dounce homogenization in 1 ml of hypotonic buffer (10 mM Tris-Cl [pH 8.0], 1 mM EDTA) with protease inhibitors and then centrifuged at 1,000 × *g* for 10 min to remove nuclei and unbroken cells. Supernatants containing cytosolic components and cellular membranes were subjected to ultracentrifugation at 100,000 × *g* for 30 min at 4°C. Soluble fractions and membrane pellets were analyzed by fluorescence spectrophotometry. Supernatants and pellets were adjusted to 0.5% Triton X-100 in NTE buffer prior to measurement, and vigorous vortexing or pipetting was performed to ensure uniform resuspension of pelleted components. Standards of serially diluted recombinant enhanced green fluorescent protein (EGFP; Clontech) were prepared in the same solution and analyzed together with experimental samples. These standards were utilized to generate a standard curve. The fluorescence intensities of the Gag-GFP samples and of the standards were determined with a VersaFluor Fluorometer (Bio-Rad, Hercules, Calif.), with excitation and emission filters being 450 nm and 510 nm, respectively. The percentage of sedimented Gag protein in each experiment was calculated as the amount of protein in the membrane pellet/(the amount of protein in the pellet plus the amount of protein in the soluble fraction).

Subcellular fractionation into detergent-resistant complexes. Cells were transfected and harvested as described above, with the following modifications. S1 supernatants were adjusted to 0.5% Triton X-100 prior to the centrifugation step. After centrifugation at 100,000 × *g*, the membranes and the proteins associated with those membranes were found in the soluble fraction, leaving detergent-resistant components in the pellet fraction. Quantitation was performed by fluorescence spectrophotometry as described above.

Electron microscopy. Gag-GFP fusion proteins were expressed as described above. Cells were harvested 12 h following transfection and fixed in 2% gluteraldehyde in phosphate buffer, postfixed with 1% osmium tetroxide, stained with 1% uranyl acetate, dehydrated in ethanol, and embedded in Spurr resin. Thin sections were cut with an ultramicrotome and analyzed on a Philips model 3000 electron microscope. In this manner, the following five Gag-GFP expression constructs were examined for particle formation: 55GAG/GFP, GAG384/GFP, GAG384(R380,384A)/GFP, GAG377/GFP, and MA/GFP. The entire grid, representing hundreds of individual fields, was examined for each construct.

RESULTS

Identification of the minimal I domain within the N-terminal subdomain of NC. In order to identify the minimal region within the N-terminal subdomain of NC that contains I domain function, a panel of Gag truncation constructs fused to GFP was generated (Fig. 1). Gag-GFP particles were harvested from cellular supernatants, pelleted through a 20% sucrose cushion, and subjected to equilibrium density centrifugation on a linear sucrose gradient. Equal fractions were collected, immunoprecipitated with pooled HIV patient sera, and analyzed

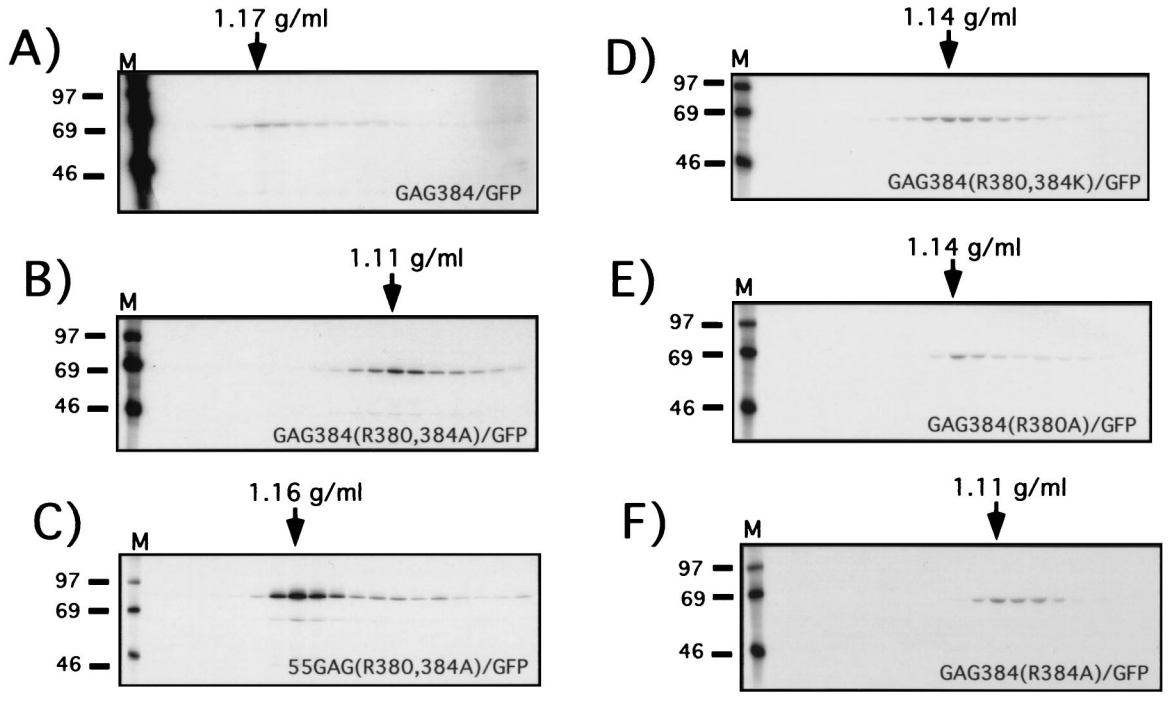

FIG. 3. Effect of mutation of arginine residues 380 and 384 upon particle density. The density of the Gag-GFP particles for the N-terminal I domain mutants was determined as described in the legend for Fig. 2. The effects of site-directed mutagenesis of R380 and R384 were examined in the context of truncated Gag (GAG384/GFP) and in the context of full-length Gag (55GAG/GFP). (A) GAG384/GFP; (B) GAG384(R380/384A)/GFP; (C) 55GAG(R380/384A)/GFP; (D) GAG384(R380/384K)/GFP; (E) GAG384(R380A)/GFP; (F) GAG384(R384A)/GFP. Arrows, peak fractions (with densities as indicated).

using SDS-PAGE. It should be noted that the gradients shown are representative of at least two independent experiments. 55GAG/GFP produced particles with a peak density of 1.17 g/ml (Fig. 2A), consistent with an earlier report by members of our group (29). MA/GFP, which consists of the matrix region fused to GFP, was released, pelleted through sucrose, and reached an equilibrium density of 1.13 g/ml (Fig. 2B). GAG377/GFP, which contains the MA, CA, and SP1 regions of Gag fused to GFP, was demonstrated to form particles of a similar light density of 1.13 g/ml (Fig. 2C). The inclusion of the N-terminal seven amino acids of NC (amino acids 378 to 384 [Fig. 1]) produced a dramatic shift in Gag-GFP particle density. GAG384/GFP produced particles of a normal density, 1.17 g/ml (Fig. 2D). Scanning densitometry of the autoradiograms derived from GAG384/GFP and GAG377/GFP particle gradients was employed to illustrate the clear separation between the peak fractions of GAG377/GFP and GAG384/GFP (Fig. 2E). The peak for dense particles was found in fractions 5 to 7, corresponding to a density of 1.17 to 1.16 g/ml; the peak for light particles was found in fractions 9 to 11, corresponding to a density of 1.13 to 1.12 g/ml. The sucrose densities from each fraction of the experiments represented in Fig. 2C and D are nearly identical, as indicated in Fig. 2E by overlap of their plotted densities. The shift in production of particles with a light density to that of a normal density therefore occurred with the addition of the N-terminal seven amino acids of NC. Based on the definition of the I domain as a density determinant, this small region in NC constitutes a functional I domain.

Characterization of the N-terminal I domain. Several previous reports have demonstrated that the N-terminal basic region of NC is of particular importance in the assembly and release of HIV particles (14, 18, 20). Basic residues placed C-terminal to CA have been shown to be sufficient to restore particle density to an RSV Gag construct lacking the I domain (2). We noted that the sequence of the minimal I domain defined above (^{378}MQRGNFR^{384}) includes two arginine residues. To examine the importance of these residues in the function of the I domain, R380 and R384 were mutated to alanine either singly or together. The double mutant was constructed in the context of both the minimal I domain construct, GAG384/GFP, and the full-length construct 55GAG/GFP, resulting in the constructs GAG384(R380,384A)/GFP and 55GAG(R380,384A)/GFP, respectively. Each arginine was also mutated individually in the context of GAG384/GFP, resulting in the constructs Gag384(R380A)/GFP and Gag384 (R384A)/GFP. To test for I domain function of these mutants, the density of the released Gag-GFP particles was determined by equilibrium density centrifugation. Parental GAG384/GFP particles peaked at a normal density of 1.17 g/ml (Fig. 3A shows the results from an experiment separate from that whose results are pictured in Fig. 2D). Mutation of the two arginine residues in the context of GAG384/GFP had a dramatic affect on the particle density. GAG384(R380,384A)/GFP, which contains the double mutation, produced particles of a very light density, 1.11 g/ml (Fig. 3B). 55GAG(R380,384A)/GFP, the construct containing the double mutation in the context of the full-length Gag, produced particles of normal density (1.16 g/ml) (Fig. 3C). This result demonstrates that I domain function is redundant within NC, which is consistent with previous findings (1, 2, 29). However, in repeated experiments, the particles produced by 55GAG(R380,384A)/GFP never attained the peak density of the 55GAG/GFP particles (1.17 g/ml), suggesting that even in this context the loss of the N-terminal I domain slightly altered the packing of Gag molecules.

Our results suggested that arginine 380 and arginine 384 play a crucial role in N-terminal I domain function. To exam-

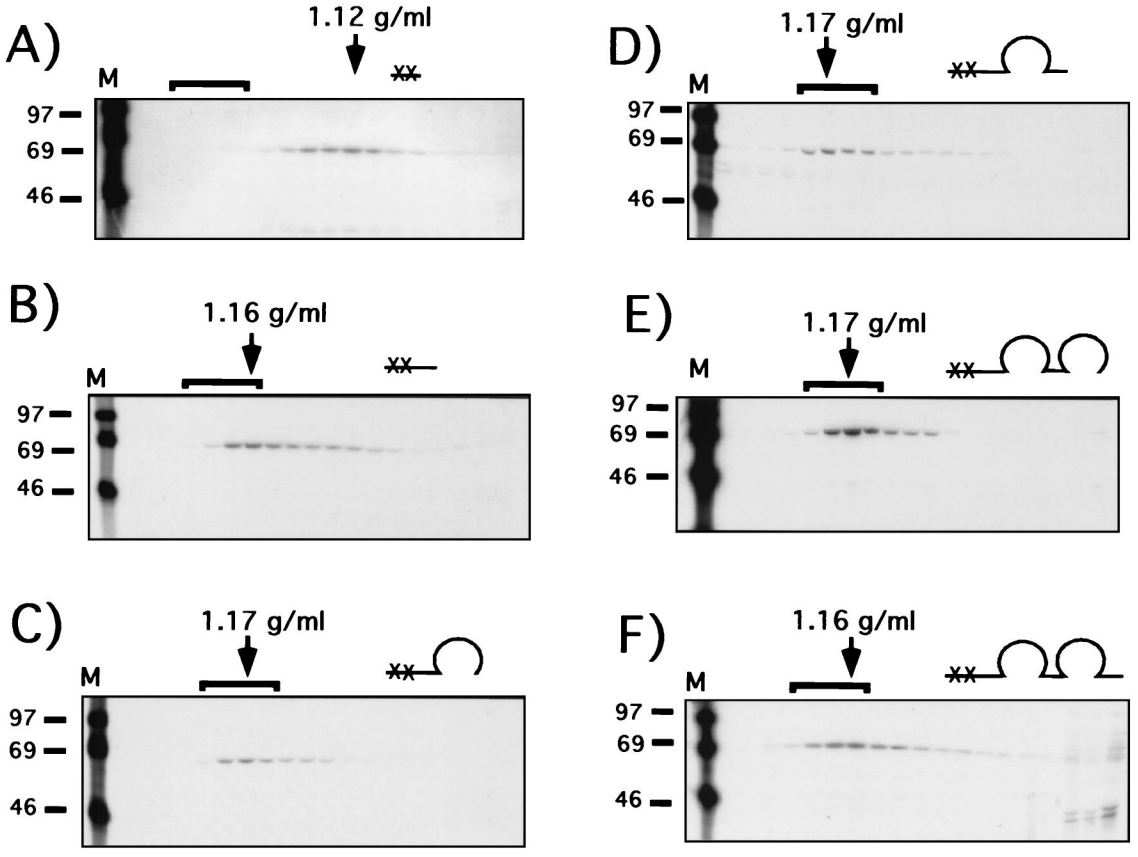

FIG. 4. Determination of buoyant density of NC N-terminal I domain mutants. The density of the Gag-GFP particles was determined as described in the legend for Fig. 2. The line diagrams above the autoradiograms represent regions of NC included in the representative construct; each pair of X's denotes the arginine-to-alanine double mutation (R380,384A). Each bracket denotes the fractions associated with dense RVLPs (1.16 to 1.18 g/ml), and the arrows indicate the peak fractions (the corresponding sucrose density is provided). Lanes M, molecular mass markers (molecular mass in kilodaltons is indicated at the left). (A) GAG384(R380/384A)/GFP; (B) GAG391(R380/384A)/GFP; (C) GAG405(R380/384A)/GFP; (D) GAG411(R380/384A)/GFP; (E) GAG426(R380/384A)/GFP; (F) GAG432(R380/384A)/GFP.

ine whether a positive charge in positions 380 and 384 is sufficient for I domain function, both arginines were changed to lysine in the context of the Gag384/GFP construct, generating Gag384(R380,384K)/GFP. The particles produced from this construct demonstrated an intermediate density of 1.14 g/ml (Fig. 3D). Individual arginine-to-lysine mutations at these positions were not examined. Thus, the presence of positive charge itself in these positions was not sufficient to restore normal retroviral particle density. Next, individual arginine-to-alanine mutations were examined for effects on particle density in the context of GAG384/GFP. GAG384(R380A)/GFP produced particles of an intermediate density, 1.14 g/ml, whereas Gag384(R384A)/GFP produced particles of a light density, 1.11 g/ml (Fig. 3E and F, respectively).

Localization of the C-terminal I domain. In order to identify additional regions within NC harboring I domain function, sequential additions of NC subdomains were constructed in the context of N-terminal I domain mutations. The R380,384A mutations were introduced into the set of NC truncation constructs shown in Fig. 1, generating the following constructs: GAG391(R380,384A)/GFP, which contains the N-terminal region of NC; GAG405(R380,384A)/GFP, which includes the addition of the first zinc finger; GAG411Gag(R380,384A)/GFP, which includes the addition of the basic linker region; GAG426(R380,384A)/GFP, which includes the addition of the second zinc finger; and GAG432(R380,384A)/GFP, which contains the entire NC region. Using particle density as an assessment of I domain function, we sought to determine which region of NC, when added back to the minimal I domain mutant, would restore dense particle formation. The results are shown in Fig. 4. GAG384(R380,384A)/GFP particles attained a light equilibrium density as has already been shown in this report (Fig. 4A; these results are from a separate experiment from that represented in Fig. 3B and are included to facilitate comparisons with the autoradiograms in Fig. 4B through F). Addition of the remaining portion of the N-terminal region of NC partially restored dense particle formation (Fig. 4B). Although the peak reached a normal density of 1.16 g/ml, the particle band was quite broad in repeated experiments and extended into the light-density range (Fig. 4B). There are three basic residues in the region that was added between positions 384 and 391, again suggesting that basic charge may have played some role in enhancing particle density. With the addition of the first zinc finger, GAG405 (R380,384A)/GFP, the particle density was restored to normal (Fig. 4C). Further addition of the basic linker region, the second zinc finger, and the C-terminal subdomain of NC did not significantly alter particle density (Fig. 4D to F).

Role of the I domain in formation of detergent-resistant Gag protein complexes. Previous results generated in our laboratory have demonstrated that the I domain contributes substantially to the efficiency of membrane binding as measured by

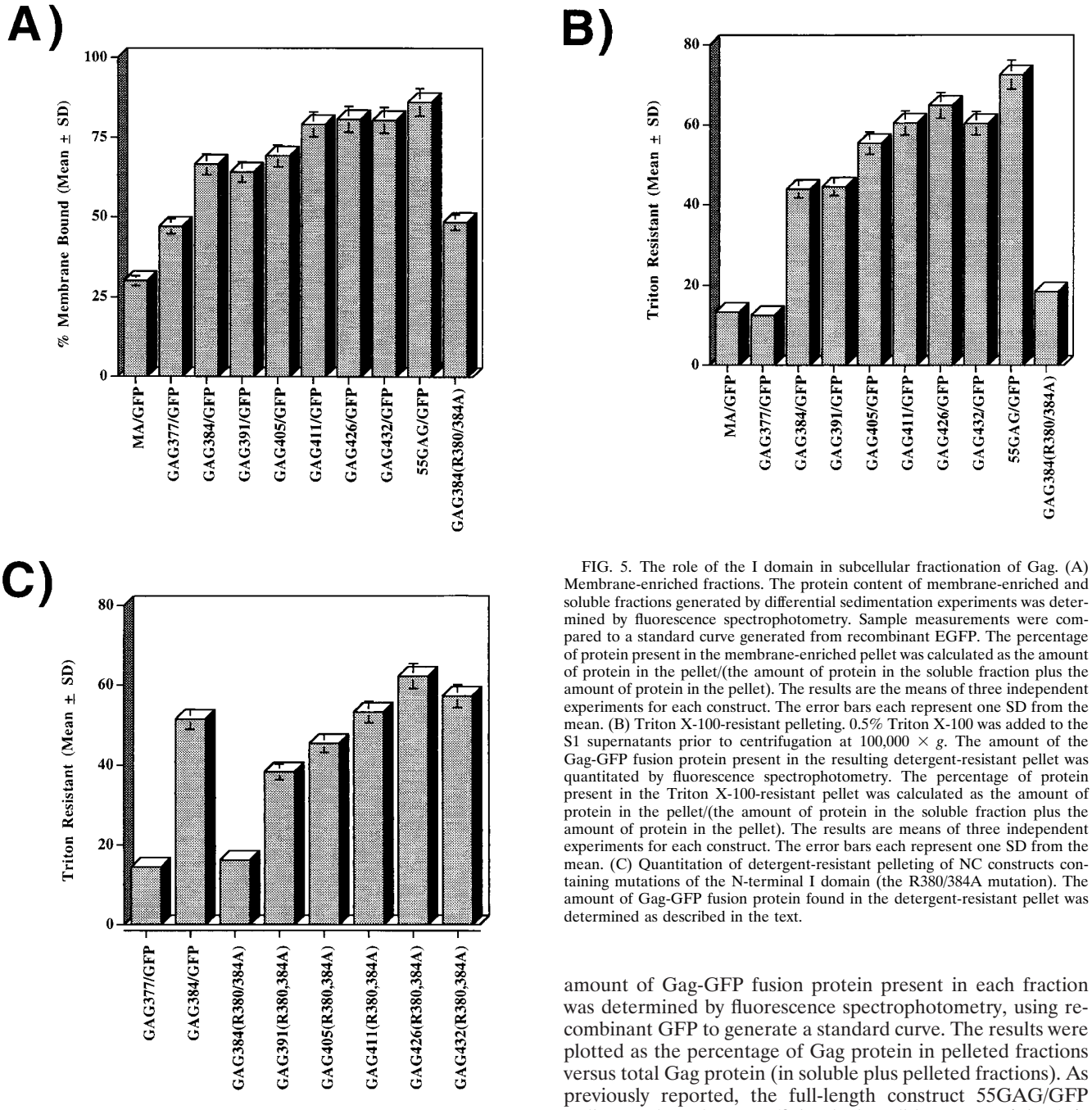

FIG. 5. The role of the I domain in subcellular fractionation of Gag. (A) Membrane-enriched fractions. The protein content of membrane-enriched and soluble fractions generated by differential sedimentation experiments was determined by fluorescence spectrophotometry. Sample measurements were compared to a standard curve generated from recombinant EGFP. The percentage of protein present in the membrane-enriched pellet was calculated as the amount of protein in the pellet/(the amount of protein in the soluble fraction plus the amount of protein in the pellet). The results are the means of three independent experiments for each construct. The error bars each represent one SD from the mean. (B) Triton X-100-resistant pelleting. 0.5% Triton X-100 was added to the S1 supernatants prior to centrifugation at 100,000 × *g*. The amount of the Gag-GFP fusion protein present in the resulting detergent-resistant pellet was quantitated by fluorescence spectrophotometry. The percentage of protein present in the Triton X-100-resistant pellet was calculated as the amount of protein in the pellet/(the amount of protein in the soluble fraction plus the amount of protein in the pellet). The results are means of three independent experiments for each construct. The error bars each represent one SD from the mean. (C) Quantitation of detergent-resistant pelleting of NC constructs containing mutations of the N-terminal I domain (the R380/384A mutation). The amount of Gag-GFP fusion protein found in the detergent-resistant pellet was determined as described in the text.

differential sedimentation centrifugation (29). However, these previous experiments did not examine the effect of the I domain upon Gag protein sedimentation in the presence of detergents. For Gag proteins, this may be particularly important, as intracellular Gag protein complexes which are resistant to detergent have been identified within HIV-infected cells and have been recently proposed to represent assembly intermediate structures (21, 22). We therefore performed experiments to determine if the I domain is responsible for the formation of detergent-resistant complexes of Gag protein. Membrane- and cytoskeleton-enriched fractions were separated from cytosolic components by differential sedimentation centrifugation following osmotic lysis in the absence of detergent. The precise amount of Gag-GFP fusion protein present in each fraction was determined by fluorescence spectrophotometry, using recombinant GFP to generate a standard curve. The results were plotted as the percentage of Gag protein in pelleted fractions versus total Gag protein (in soluble plus pelleted fractions). As previously reported, the full-length construct 55GAG/GFP sedimented much more efficiently than did MA/GFP (Fig. 5A). Extension of the Gag sequence to include MA, CA, and SP1 (GAG377/GFP) led to a small increase in the percentage of Gag protein in the membrane-enriched pellet. Addition of the seven amino acids of the N-terminal I domain (represented by GAG384/GFP) led to a significant increase in the percentage of sedimented Gag protein ($P = 0.012$ by Student's t test for GAG377/GFP versus GAG384/GFP). There was not a significant further increase in the differential sedimentation results for the remaining constructs, although the mean percentages were slightly higher for GAG411/GFP, GAG426/GFP, GAG432/GFP, and 55GAG/GFP.

The pellet generated from differential sedimentation centrifugation contains not only the cellular membranes but also cytoskeletal proteins and any cellular components with a high

sedimentation value. Complexes of Gag protein which would also sediment in these conditions may form intracellularly. To determine what portion of the Gag protein found in the membrane- and cytoskeleton-enriched pellet was due to membrane binding versus cytoskeletal binding or Gag protein complex formation, 0.5% Triton X-100 was added to the S1 supernatant prior to centrifugation at 100,000 × *g*. The detergent solubilizes the membranes, and membrane-associated proteins are thus shifted to the soluble fraction. Very little MA/GFP was found in the detergent-resistant pellet. Extension of the Gag sequence to include MA, CA, and SP1 (GAG377/GFP) did not significantly alter the amount of Gag protein found in the detergent-resistant fraction (Fig. 5B). Addition of the N-terminal I domain, however, significantly increased the percentage of protein found in the detergent-resistant pellet ($P = 0.001$ by Student's t test for GAG377/GFP versus GAG384/GFP). There was a further increase in the mean amount of detergent-resistant Gag protein upon the addition of the first zinc finger (GAG405/GFP). This result is consistent with the finding that inclusion of the first zinc finger was able to restore dense particle formation to the N-terminal I domain mutant (Fig. 4) and suggests that the two phenomena may be linked. The efficiency with which Gag proteins sedimented in the presence of detergent increased sequentially upon addition of the first zinc finger (GAG405/GFP), the basic linker region (GAG411/GFP), and the second zinc finger (GAG426/GFP). However, differences in the efficiency of sedimentation between GAG405/GFP, GAG411/GFP, and GAG426/GFP did not reach statistical significance. Addition of the C-terminal region of NC (GAG432/GFP) decreased the amount of detergent-resistant pelleting slightly, although this difference also did not reach statistical significance ($P = 0.474$ by Student's t test for GAG426/GFP versus GAG432/GFP). The efficient sedimentation of Gag in the presence of nonionic detergent thus correlated closely with I domain function as determined by the density of released particles.

Mapping the domains within NC that contribute to detergent-resistant complex formation. In order to determine which of the subdomains of NC contributes to the ability of Gag to form detergent-resistant complexes, we utilized the constructs already described which contain an R380,384A substitution. These constructs were expressed in BSC-40 cells, and differential sedimentation was performed following the addition of Triton X-100. The R380,384A mutations that were noted to disrupt I domain function in the density assays also dramatically altered the ability of the Gag-GFP fusion protein to sediment in the detergent-resistant pellet [as shown by a comparison of the results for GAG384/GFP and GAG384(R380,384A)/GFP (Fig. 5C)]. GAG384(R380,384A)/GFP showed a marked decrease in the detergent-resistant pelleting compared to wild-type GAG384/GFP, from a mean of 44% for the wild type to 18% for the mutant, which is similar to I domain-deficient constructs (MA/GFP and GAG377/GFP). Next we measured the amount of Gag-GFP fusion protein found in the detergent-resistant pellet for constructs representing the addition of individual subdomains of NC in the context of the N-terminal I domain mutations (Fig. 5C). Addition of the remaining portion of the N-terminal region of NC (GAG391(R380,384A/GFP) led to an increase in sedimented Gag protein; however, it was still significantly lower than GAG384/GFP with an intact N-terminal I domain segment. The addition of the first zinc finger [GAG405(R380,384A)/GFP] resulted in levels of detergent-resistant pelleting comparable to the levels of GAG384/GFP. A stepwise increase in the percentage of the fusion protein was found in the detergent-resistant pellet upon expression of each additional subdomain of NC in the construct, with the exception of the C-terminal domain [represented by GAG432(R380,384A)/GFP]. It is interesting to note that only with the addition of the second zinc finger [GAG426(R380,384A)/GFP] does the percentage of protein in the detergent-resistant pellet reach the maximum value seen for this series of Gag truncation constructs, suggesting that the effects of each subdomain upon formation of Gag protein detergent-resistant complexes were additive.

Subcellular localization of Gag proteins visualized by confocal microscopy. Members of our group have previously noted that Gag-GFP constructs containing an I domain are found in distinct foci underlying the plasma membrane, while Gag-GFP constructs lacking the I domain are distributed more diffusely within the cellular cytoplasm (29). We reasoned that if altered cellular distribution represents a true function contributed by the I domain, then a redistribution of Gag protein would be apparent for mutants that disrupt the function of the N-terminal I domain. Laser confocal microscopy was performed to examine the localization of the Gag-GFP fusion protein constructs in living cells (Fig. 6). Constructs that lacked the I domain demonstrated a diffuse distribution throughout the cytoplasm of the cell. This was apparent for all constructs lacking the I domain as previously reported (MA/GFP, GAGP/GFP, and MACA/GFP [29]), and is represented in Fig. 6A by GAG377/GFP. Addition of the N-terminal I domain resulted in a transition to plasma membrane localization (GAG384/GFP [Fig. 6B]). We noted that for the minimal I domain construct, GAG384/GFP, the membrane localization is not complete. There is a fraction of diffuse, cytoplasmic localization and a fraction of punctate, peripheral membrane localization (Fig. 6B). Expression of additional subdomains within NC resulted in more complete plasma membrane localization, as demonstrated by GAG426/GFP (Fig. 6C). These results are consistent with previous findings (29) and appear to correlate with the amount of Gag protein present in detergent-resistant complexes (i.e., those constructs with the highest percentage of detergent-resistant complex demonstrate a higher percentage of peripheral, punctate Gag protein). Next, we sought to determine the effect of the N-terminal I domain mutations on the localization of the Gag-GFP fusion protein. Cells expressing GAG384(R380,384A)/GFP demonstrated a diffuse, cytoplasmic distribution of the protein (Fig. 6D). Therefore, disruption of the I domain not only alters particle density, it also affects Gag protein subcellular localization as revealed by confocal microscopy. Addition of the remaining segment of the N-terminal region of NC and the N-terminal zinc finger led to a redistribution of Gag to distinct foci at the plasma membrane [GAG405(R380,384A)/GFP (Fig. 6E)]. This result is consistent with the finding that the first zinc finger restored dense particle formation and detergent-resistant complex formation to the N-terminal I domain mutant. These observations suggest that the effects of the I domain upon particle density, detergent-resistant complex formation, and the presence of Gag in focal sites at the plasma membrane are tightly linked.

RVLP formation elicited by Gag-GFP fusion constructs. In order to determine the morphology of the light and dense retroviral particles described in this study, electron microscopic analysis of cells expressing representative constructs was performed. 55GAG/GFP expression yielded retrovirus-like particles that were readily detected budding from the plasma membrane of cells (Fig. 7A). The particles were 120 to 140 nm in diameter, slightly larger than the expected size of 110 to 130 nm. In many of the examined sections, 55GAG/GFP particles demonstrated an irregular dense border which suggested clumping of the Gag-GFP protein around the perimeter of the immature particles (Fig. 7B). The expression construct con-

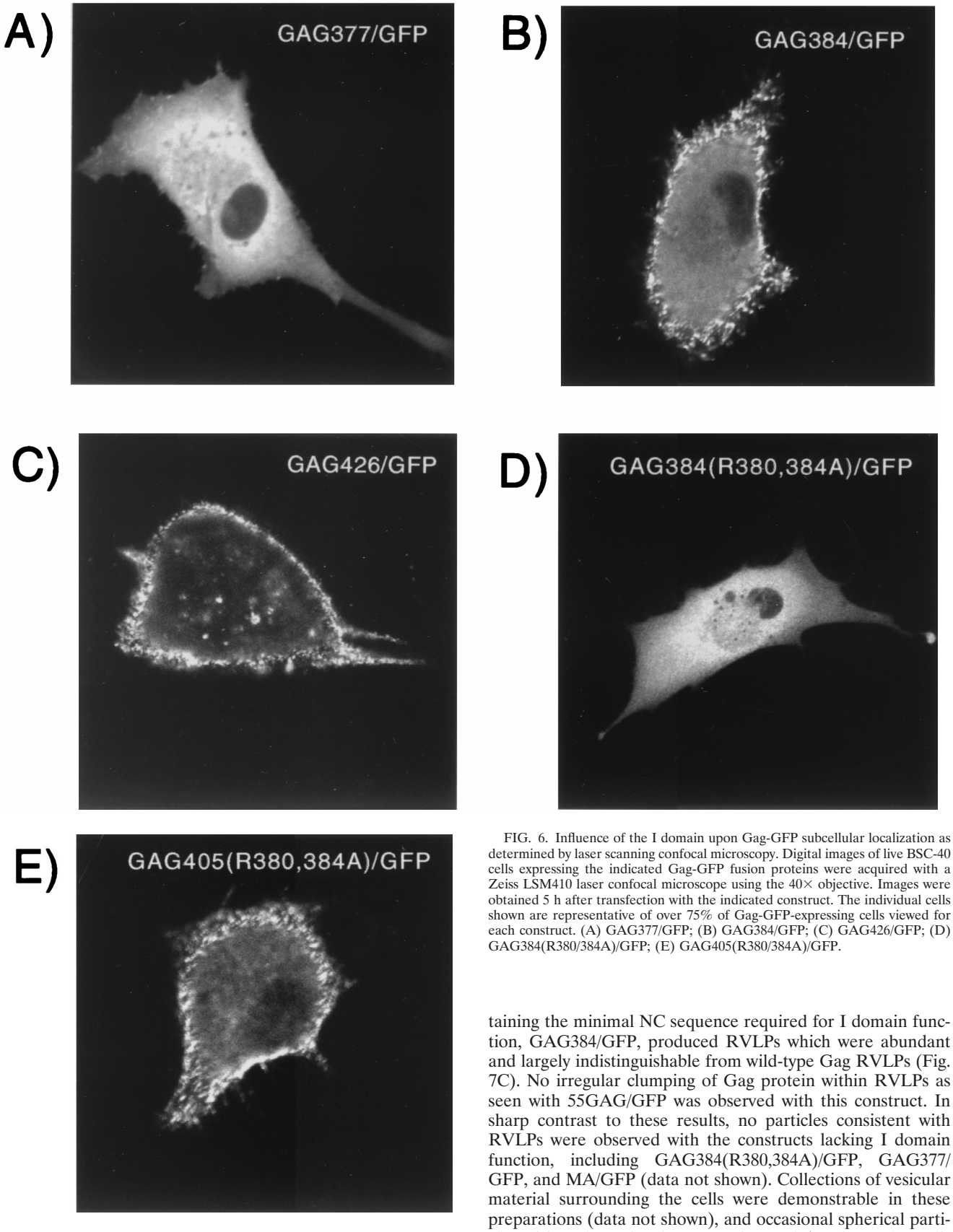

FIG. 6. Influence of the I domain upon Gag-GFP subcellular localization as determined by laser scanning confocal microscopy. Digital images of live BSC-40 cells expressing the indicated Gag-GFP fusion proteins were acquired with a Zeiss LSM410 laser confocal microscope using the 40× objective. Images were obtained 5 h after transfection with the indicated construct. The individual cells shown are representative of over 75% of Gag-GFP-expressing cells viewed for each construct. (A) GAG377/GFP; (B) GAG384/GFP; (C) GAG426/GFP; (D) GAG384(R380/384A)/GFP; (E) GAG405(R380/384A)/GFP.

taining the minimal NC sequence required for I domain function, GAG384/GFP, produced RVLPs which were abundant and largely indistinguishable from wild-type Gag RVLPs (Fig. 7C). No irregular clumping of Gag protein within RVLPs as seen with 55GAG/GFP was observed with this construct. In sharp contrast to these results, no particles consistent with RVLPs were observed with the constructs lacking I domain function, including GAG384(R380,384A)/GFP, GAG377/GFP, and MA/GFP (data not shown). Collections of vesicular material surrounding the cells were demonstrable in these preparations (data not shown), and occasional spherical particles with a dense border were observed (as shown for cells expressing MA/GFP in Fig. 7D). Notably, these particles were

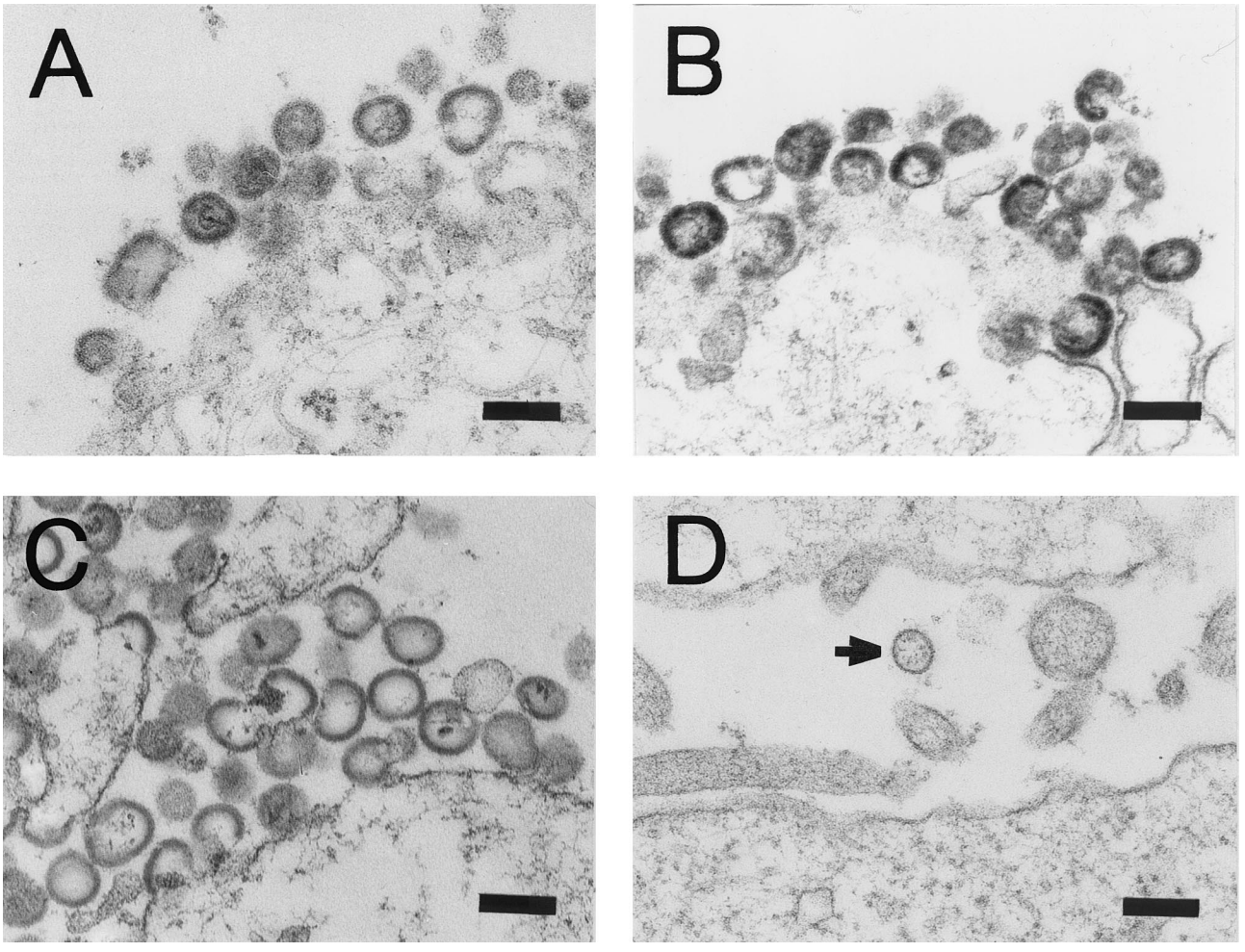

FIG. 7. Electron microscopy of Gag-GFP particles. (A) 55GAG/GFP; (B) 55GAG/GFP; (C) GAG384/GFP; (D) MA/GFP. Arrow indicates particle of uncertain nature discussed in Results. Magnification, ×51,250. Bar = 195 nm.

smaller in diameter (90 to 100 nm) and lacked the thick peripheral layer of Gag protein typical of Gag RVLPs (Fig. 7, compare panels C and D). The association of these atypical particles with Gag protein was not proven in the present study. In order to determine if our inability to demonstrate RVLP production by I domain-deficient Gag was merely due to inefficient particle release, the amount of Gag-GFP protein released from cells expressing four of the Gag-GFP constructs was measured by microplate fluorometry. With the amount of released 55GAG/GFP set at 100% as a reference value, the following results were obtained (means ± standard deviations [SD] from three separate experiments): for GAG432/GFP, 22% ± 8%; for GAG384/GFP, 19 ± 11%; for GAG377/GFP, 13.2% ± 8%; and for MA/GFP, 12 ± 6%. Because the amount of released Gag protein differed only twofold between an I domain-containing construct that demonstrated numerous RVLPs by electron microscopy (GAG384/GFP) and those demonstrating no evident RVLPs (GAG377/GFP and MA/GFP), it is unlikely that inefficient production or release accounted for the absence of observed RVLPs in this study. These results suggest that the light particles formed by Gag proteins lacking I domain function in our study may not be found associated with true RVLPs but may represent Gag proteins released in some other form (such as in association with cellular vesicles).

DISCUSSION

Localization of the N-terminal I domain. The N-terminal I domain was localized in this study to the N-terminal seven amino acids of NC. Although it is surprising that such a discrete, small domain was sufficient to confer upon the 377-amino-acid Gag molecule a dramatic shift in particle density, the existence of a domain essential for particle assembly located in the extreme N terminus of NC has been previously reported (14, 18, 20). Our results extend this finding and link this particle assembly domain to the function of the I domain. The finding that two basic residues within this small region are required for I domain function is consistent with the report that addition of a small string of basic amino acids to a truncated RSV Gag protein restored dense particle formation (2). However, substitution of lysine residues in these positions in our study failed to completely reconstitute normal particle density as predicted. These data suggest that charge alone is insufficient to reconstitute I domain function, at least in this context, or that a particular arginine (R384) may play a more specific role which is not recreated by lysine substitution. It is also interesting to note that the single substitution of R384 altered particle density to a greater degree than that of the single substitution of R380. R384 (R7 in the NCp7 protein) has recently been shown to make critical electrostatic interactions

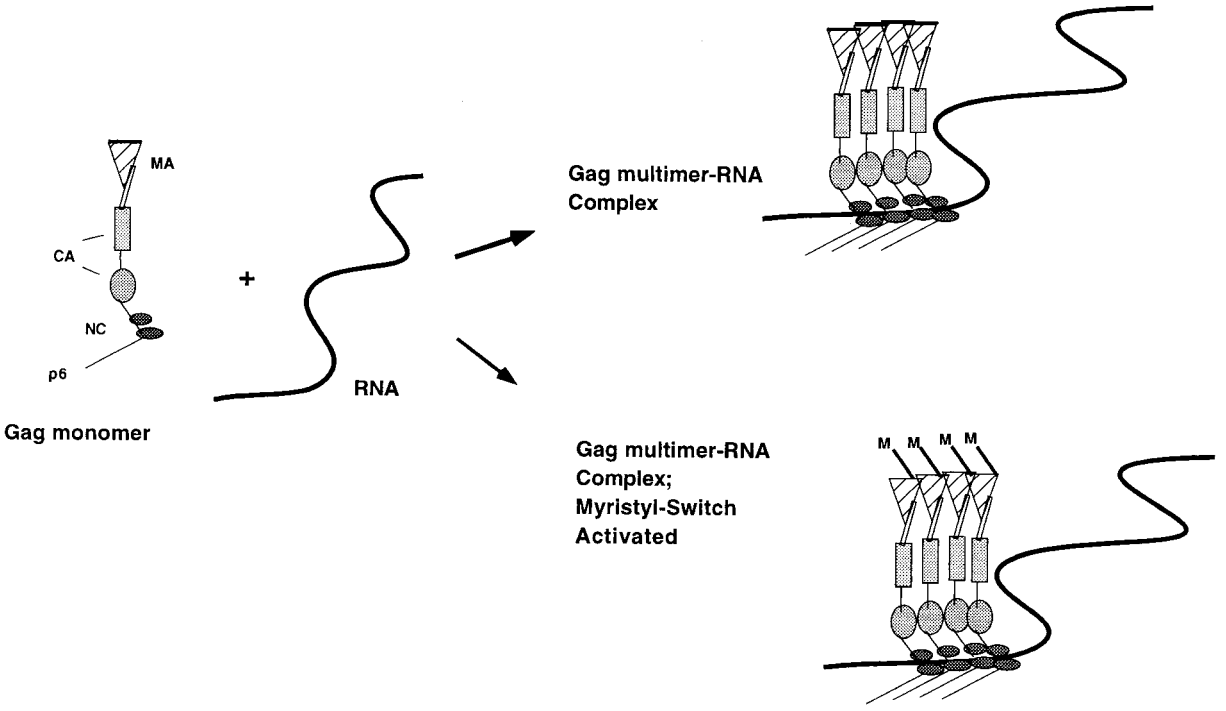

FIG. 8. Proposed model for I domain function. Gag monomers bind to an RNA molecule through the I domain, which is located in multiple subdomains of NC. The RNA then acts as a tether to allow Gag-Gag multimerization to take place. Multimerization creates an intermediate structure that has enhanced membrane binding energy by bringing together multiple M domains in a common orientation (top right). An alternative possibility to explain enhanced membrane association is illustrated on the bottom right. According to this model, the myristyl switch within MA is triggered through the influence of the I domain, making myristic acid available for membrane interactions.

with a homopolymeric RNA template by fluorescence spectroscopy (33), and it is possible that this interaction is important in I domain function.

I domain and Gag protein detergent-resistant complex formation. The ability of Gag to form intracellular Triton X-100-resistant complexes has recently been identified in HIV-infected cells and is proposed to represent an assembly intermediate (21, 22). Data from the present study indicate that detergent resistance is mediated by the I domain. In the presence of N-terminal I domain mutants, detergent-resistant sedimentation is enhanced sequentially by the addition of further subdomains of NC, including the addition of the remainder of the N-terminal subdomain, the N-terminal zinc finger, the basic linker region, and the second zinc finger. Taken together, these data suggest that I domain function in the intact Gag polyprotein is contributed by each of these four subdomains of NC. A threshold amount of I domain activity is required to allow particles of normal density to form; this may be contributed by the N-terminal I domain alone or by the N-terminal zinc finger in the absence of N-terminal I domain activity. Additional combinations of I domain functional units from subdomains other than the N-terminal I domain and the first zinc finger, must also be sufficient based upon data from studies with RSV-HIV Gag chimeric proteins (1). Thus, there are at least three functional I domain units within HIV-1 NC.

I domain and Gag subcellular localization. The contribution of the I domain to Gag protein subcellular localization in our studies is somewhat enigmatic. It is clear that the M domain is required for plasma membrane localization of Gag, yet the I domain enhanced the peripheral localization of Gag dramatically in these studies. However, disruption of the M domain by elimination of the myristylation site abolishes any apparent contribution of the I domain to peripheral localization of Gag (29). These findings are best reconciled by the hypothesis that while the M domain is required for membrane localization of Gag, the I domain enhances the efficiency of membrane interaction or acts to stabilize the interaction. This may occur through cooperative effects upon membrane binding: as multiple Gag molecules interact in a coordinated fashion, a membrane-binding unit of enhanced binding energy is formed (illustrated in Fig. 8). In the absence of the I domain, the weak membrane-binding energy of Gag monomers is insufficient to maintain the interaction and the molecule dissociates from the membrane. Alternatively, the I domain may act to provide a trigger for the myristyl switch present within MA. According to this hypothesis, Gag-Gag interactions contributed by the I domain lead to a conformational change within MA. The conformational change then results in a more favorable presentation of myristic acid for membrane interaction (Fig. 8). Several groups have now provided supporting data for the presence of the myristyl switch within MA (25, 26, 30, 43). However, it remains to be demonstrated how direct Gag-Gag interactions, which are most likely mediated by the CA-CA dimer interface, with a possible contribution from NC (3, 9), could result in a conformational change in the M domain. Solved structures of MA reveal a long C-terminal helix through which such a conformational change would have to be transmitted (17, 24), and cryoelectron microscopy studies have demonstrated a significant distance (approximately 70 Å) between the radial densities corresponding to the MA globular domain and the C-terminal domain of CA (11).

Nature of light Gag particles. The nature of the Gag particles lacking I domains (such as GAG377/GFP and MA/GFP) is not clear. We and others have previously shown that HIV-1

Gag constructs lacking all of NC are released, sediment through a sucrose cushion, and attain an equilibrium density of 1.10 to 1.14 g/ml when analyzed by equilibrium density centrifugation (6, 29, 41), and these results agree with the description of light particles produced by RSV Gag in the absence of the I domain (1). It should be noted that the efficiency of particle release in the absence of NC is diminished (6, 41). In this study, we failed to demonstrate by electron microscopy any apparent RVLPs budding from cells expressing truncated Gag-GFP proteins that lack the I domain, a result which could not be accounted for by observed differences in the amount of Gag released. This striking lack of RVLP formation suggests that for HIV-1 Gag, the I domain may be a required domain for RVLP formation itself. The released Gag protein of light density may represent Gag protein associated with cellular microvesicles, a hypothesis worthy of further study. Alternatively, Gag proteins lacking the I domain may form aberrant particles that lack the characteristic electron microscopic appearance of RVLPs.

Role of RNA binding in I domain function. In vitro models of retroviral particle assembly have implicated the RNA binding function within NC as an important determinant of particle assembly (4, 5). Also in support of a critical role for RNA is a recent report that Gag-Gag multimerization requires RNA interaction and that RNase can disrupt Gag-Gag interaction in vitro (3). We favor a model of I domain function in which RNA binding is contributed by the I domain, and RNA binding then facilitates Gag-Gag multimerization. The RNA binding relevant to the present study must be nonspecific binding, as our Gag constructs did not include the RNA packaging (*psi*) region of the genome. The fact that the R384 residue which was shown here to be important for N-terminal I domain function has been identified as one of four key residues within NC involved in critical electrostatic contacts with a homopolymeric RNA template supports this model. Additional key residues for nonspecific RNA binding are located within the N-terminal zinc finger and the C-terminal zinc finger (33). Taken together, our data fit with a model in which multiple regions of NC act concomitantly to bind RNA and in which RNA binding then facilitates Gag-Gag interaction and dense particle formation. Further investigation into the mechanism by which the I domain contributes to dense particle formation will be needed and is expected to yield important insights into the assembly process of retroviruses.

ACKNOWLEDGMENTS

We acknowledge the Cell Imaging Core Laboratory of the Vanderbilt-Ingram Cancer Center at Vanderbilt University for assistance with confocal microscopy, the Sequencing Core Laboratory of the Vanderbilt-Ingram Cancer Center for assistance with automated sequencing of expression plasmid inserts, and the Electron Microscopy Laboratory of the Department of Pathology at Vanderbilt University for assistance with obtaining electron micrographs. We thank Terry Dermody for critical evaluation of this manuscript prior to submission. Plasmid pHIV-gpt was obtained from Kathleen Page and Dan Littman through the NIH AIDS Research and Reference Reagent Program.

This work was supported by NIH grants AI40338 (P.S.), AI44369 (P.S.), and AI45210 (V.V. and S.S.).

REFERENCES

1. **Bennett, R. P., T. D. Nelle, and J. W. Wills.** 1993. Functional chimeras of the Rous sarcoma virus and human immunodeficiency virus Gag proteins. J. Virol. **67:**6487–6498.
2. **Bowzard, J. B., R. P. Bennett, N. K. Krishna, S. M. Ernst, A. Rein, and J. W. Wills.** 1998. Importance of basic residues in the nucleocapsid sequence for retrovirus Gag assembly and complementation rescue. J. Virol. **72:**9034–9044.
3. **Burniston, M. T., A. Cimarelli, J. Colgan, S. P. Curtis, and J. Luban.** 1999. Human immunodeficiency virus type 1 Gag polyprotein multimerization requires the nucleocapsid domain and RNA and is promoted by the capsid-dimer interface and the basic region of matrix protein. J. Virol. **73:**8527–8540.
4. **Campbell, S., and A. Rein.** 1999. In vitro assembly properties of human immunodeficiency virus type 1 Gag protein lacking the p6 domain. J. Virol. **73:**2270–2279.
5. **Campbell, S., and V. M. Vogt.** 1995. Self-assembly in vitro of purified CA-NC proteins from Rous sarcoma virus and human immunodeficiency virus type 1. J. Virol. **69:**6487–6497.
6. **Dawson, L., and X. F. Yu.** 1998. The role of nucleocapsid of HIV-1 in virus assembly. Virology **251:**141–157.
7. **Dorfman, T., A. Bukovsky, A. Ohagen, S. Hoglund, and H. G. Gottlinger.** 1994. Functional domains of the capsid protein of human immunodeficiency virus type 1. J. Virol. **68:**8180–8187.
8. **Erdie, C. R., and J. W. Wills.** 1990. Myristylation of Rous sarcoma virus Gag protein does not prevent replication in avian cells. J. Virol. **64:**5204–5208.
9. **Franke, E. K., H. E. Yuan, K. L. Bossolt, S. P. Goff, and J. Luban.** 1994. Specificity and sequence requirements for interactions between various retroviral Gag proteins. J. Virol. **68:**5300–5305.
10. **Freed, E. O.** 1998. HIV-1 gag proteins: diverse functions in the virus life cycle. Virology **251:**1–15.
11. **Fuller, S. D., T. Wilk, B. E. Gowen, H. G. Krausslich, and V. M. Vogt.** 1997. Cryoelectron microscopy reveals ordered domains in the immature HIV-1 particle. Curr. Biol. **7:**729–738.
12. **Garnier, L., J. B. Bowzard, and J. W. Wills.** 1998. Recent advances and remaining problems in HIV assembly. AIDS **12:**S5–S16.
13. **Garnier, L., L. J. Parent, B. Rovinski, S. X. Cao, and J. W. Wills.** 1999. Identification of retroviral late domains as determinants of particle size. J. Virol. **73:**2309–2320.
14. **Gheysen, D., E. Jacobs, F. de Foresta, C. Thiriart, M. Francotte, D. Thines, and M. De Wilde.** 1989. Assembly and release of HIV-1 precursor Pr55gag virus-like particles from recombinant baculovirus-infected insect cells. Cell **59:**103–112.
15. **Gitti, R. K., B. M. Lee, J. Walker, M. F. Summers, S. Yoo, and W. I. Sundquist.** 1996. Structure of the amino-terminal core domain of the HIV-1 capsid protein. Science **273:**231–235.
16. **Gottlinger, H. G., T. Dorfman, J. G. Sodroski, and W. A. Haseltine.** 1991. Effect of mutations affecting the p6 gag protein on human immunodeficiency virus particle release. Proc. Natl. Acad. Sci. USA **88:**3195–3199.
17. **Hill, C. P., D. Worthylake, D. P. Bancroft, A. M. Christensen, and W. I. Sundquist.** 1996. Crystal structures of the trimeric human immunodeficiency virus type 1 matrix protein: implications for membrane association and assembly. Proc. Natl. Acad. Sci. USA **93:**3099–3104.
18. **Hoshikawa, N., A. Kojima, A. Yasuda, E. Takayashiki, S. Masuko, J. Chiba, T. Sata, and T. Kurata.** 1991. Role of the gag and pol genes of human immunodeficiency virus in the morphogenesis and maturation of retrovirus-like particles expressed by recombinant vaccinia virus: an ultrastructural study. J. Gen. Virol. **72:**2509–2517.
19. **Hunter, E.** 1994. Macromolecular interactions in the assembly of HIV and other retroviruses. Semin. Virol. **5:**71–83.
20. **Jowett, J. B., D. J. Hockley, M. V. Nermut, and I. M. Jones.** 1992. Distinct signals in human immunodeficiency virus type 1 Pr55 necessary for RNA binding and particle formation. J. Gen. Virol. **73:**3079–3086. (Erratum, **74:** 943, 1993.)
21. **Lee, Y. M., B. Liu, and X. F. Yu.** 1999. Formation of virus assembly intermediate complexes in the cytoplasm by wild-type and assembly-defective mutant human immunodeficiency virus type 1 and their association with membranes. J. Virol. **73:**5654–5662.
22. **Lee, Y. M., and X. F. Yu.** 1998. Identification and characterization of virus assembly intermediate complexes in HIV-1-infected CD4+ T cells. Virology **243:**78–93.
23. **Mammano, F., A. Ohagen, S. Hoglund, and H. G. Gottlinger.** 1994. Role of the major homology region of human immunodeficiency virus type 1 in virion morphogenesis. J. Virol. **68:**4927–4936.
24. **Massiah, M. A., D. Worthylake, A. M. Christensen, W. I. Sundquist, C. P. Hill, and M. F. Summers.** 1996. Comparison of the NMR and X-ray structures of the HIV-1 matrix protein: evidence for conformational changes during viral assembly. Protein Sci. **5:**2391–2398.
25. **Ono, A., and E. O. Freed.** 1999. Binding of human immunodeficiency virus type 1 Gag to membrane: role of the matrix amino terminus. J. Virol. **73:**4136–4144.
26. **Paillart, J.-C., and H. G. Göttlinger.** 1999. Opposing effects of human immunodeficiency virus type 1 matrix mutations support a myristyl switch model of Gag membrane targeting. J. Virol. **73:**2604–2612.
27. **Parent, L. J., R. P. Bennett, R. C. Craven, T. D. Nelle, N. K. Krishna, J. B. Bowzard, C. B. Wilson, B. A. Puffer, R. C. Montelaro, and J. W. Wills.** 1995. Positionally independent and exchangeable late budding functions of the Rous sarcoma virus and human immunodeficiency virus Gag proteins. J. Virol. **69:**5455–5460.
28. **Reicin, A. S., A. Ohagen, L. Yin, S. Hoglund, and S. P. Goff.** 1996. The role of Gag in human immunodeficiency virus type 1 virion morphogenesis and

early steps of the viral life cycle. J. Virol. **70:**8645–8652.
29. **Sandefur, S., V. Varthakavi, and P. Spearman.** 1998. The I domain is required for efficient plasma membrane binding of human immunodeficiency virus type 1 Pr55^{Gag}. J. Virol. **72:**2723–2732.
30. **Spearman, P., R. Horton, L. Ratner, and I. Kuli-Zade.** 1997. Membrane binding of human immunodeficiency virus type 1 matrix protein in vivo supports a conformational myristyl switch mechanism. J. Virol. **71:**6582–6592.
31. **Spearman, P., J. J. Wang, N. Vander Heyden, and L. Ratner.** 1994. Identification of human immunodeficiency virus type 1 Gag protein domains essential to membrane binding and particle assembly. J. Virol. **68:**3232–3242.
32. **Swanstrom, R., and J. W. Wills.** 1997. Synthesis, assembly, and processing of viral proteins, p. 263–334. *In* J. M. Coffin, S. H. Hughes, and H. E. Varmus (ed.), Retroviruses. Cold Spring Harbor Laboratory Press, Cold Spring Harbor, N.Y.
33. **Urbaneja, M. A., B. P. Kane, D. G. Johnson, R. J. Gorelick, L. E. Henderson, and J. R. Casas-Finet.** 1999. Binding properties of the human immunodeficiency virus type 1 nucleocapsid protein p7 to a model RNA: elucidation of the structural determinants for function. J. Mol. Biol. **287:**59–75.
34. **Verderame, M. F., T. D. Nelle, and J. W. Wills.** 1996. The membrane-binding domain of the Rous sarcoma virus Gag protein. J. Virol. **70:**2664–2668.
35. **von Poblotzki, A., R. Wagner, M. Niedrig, G. Wanner, H. Wolf, and S. Modrow.** 1993. Identification of a region in the Pr55gag-polyprotein essential for HIV-1 particle formation. Virology **193:**981–985.
36. **von Schwedler, U. K., T. L. Stemmler, V. Y. Klishko, S. Li, K. H. Albertine, D. R. Davis, and W. I. Sundquist.** 1998. Proteolytic refolding of the HIV-1 capsid protein amino-terminus facilitates viral core assembly. EMBO J. **17:**1555–1568.
37. **Wills, J. W., and R. C. Craven.** 1991. Form, function, and use of retroviral gag proteins. AIDS **5:**639–654.
38. **Wills, J. W., R. C. Craven, and J. A. Achacoso.** 1989. Creation and expression of myristylated forms of Rous sarcoma virus Gag protein in mammalian cells. J. Virol. **63:**4331–4343.
39. **Yoo, S., D. G. Myszka, C. Yeh, M. McMurray, C. P. Hill, and W. I. Sundquist.** 1997. Molecular recognition in the HIV-1 capsid/cyclophilin A complex. J. Mol. Biol. **269:**780–795.
40. **Zhang, W. H., D. J. Hockley, M. V. Nermut, Y. Morikawa, and I. M. Jones.** 1996. Gag-Gag interactions in the C-terminal domain of human immunodeficiency virus type 1 p24 capsid antigen are essential for Gag particle assembly. J. Gen. Virol. **77:**743–751.
41. **Zhang, Y., and E. Barklis.** 1997. Effects of nucleocapsid mutations on human immunodeficiency virus assembly and RNA encapsidation. J. Virol. **71:**6765–6776.
42. **Zhou, W., L. J. Parent, J. W. Wills, and M. D. Resh.** 1994. Identification of a membrane-binding domain within the amino-terminal region of human immunodeficiency virus type 1 Gag protein which interacts with acidic phospholipids. J. Virol. **68:**2556–2569.
43. **Zhou, W., and M. D. Resh.** 1996. Differential membrane binding of the human immunodeficiency virus type 1 matrix protein. J. Virol. **70:**8540–8548.